Analysis of the clinical value of ^{18}F-FDG PET/CT in hepatic alveolar echinococcosis before and after autologous liver transplantation

YONGDE QIN[1*], XIAOHONG LI[1*], QIZHOU ZHANG[1], BIN XIE[1], XUEWEN JI[2], YUBIN LI[1], AMINA YIBLAYAN[1] and HAO WEN[2]

Departments of [1]Nuclear Medicine and [2]Hepatobiliary Surgery, The First Affiliated Hospital of Xinjiang Medical University, Urumqi, Xinjiang Uyghur Autonomous Region 830054, P.R. China

Received August 27, 2014; Accepted June 8, 2015

DOI: 10.3892/etm.2015.2857

Abstract. The aim of this study was to evaluate the clinical value of ^{18}F-fluorodeoxyglucose (^{18}F-FDG) positron emission tomography/computed tomography (PET/CT) in advanced liver alveolar echinococcosis (LAE) prior to and following autologous liver transplantation (ALT). The biodistribution of lesions in 8 patients was recorded using ^{18}F-FDG PET/CT prior to and following surgery. The maximum standardized uptake value (SUVmax) of the lesions was also measured and compared with the pathological results. The overall hepatic peri-lesion SUVmax of the patients was 3.57±1.21, and the delayed SUVmax was 4.19±1.70. The diagnostic sensitivity of ^{18}F-FDG PET/CT in LAE was 91.67%, with a specificity of 60.00% and accuracy of 82.35%. The positive predictive value was 84.62%, and the negative predictive value was 75.00%. SUVmax values of the surviving liver were 1.23±0.78 after 1 month, 1.15±0.67 after 3 months and 0.85±0.35 after 6 months. Compared with normal liver values (0.95±0.19), the 1-month SUVmax was significantly different. The SUVmax in 3 patients with high-lividity lesions was 2.05±0.72, and the delayed SUVmax was 3.15±0.83; 3 months after transplantation, the SUVmax was 1.85±0.62, and the delayed SUVmax was 2.95±0.79, revealing no significant difference. In conclusion, ^{18}F-FDG PET/CT is effective for determining the biological boundary of LAE and shows important clinical value in determining the metabolic activities of the surviving liver following ALT.

Correspondence to: Dr Hao Wen, Department of Hepatobiliary Surgery, The First Affiliated of Xinjiang Medical University, 137 Liyushannan Road, Urumqi, Xinjiang Uyghur Autonomous Region 830054, P.R. China
E-mail: haowencn@126.com

*Contributed equally

Key words: liver alveolar echinococcosis, autologous liver transplantation, positron emission tomography, deoxyglucose

Introduction

Currently, among the various treatment methods for liver alveolar echinococcosis (LAE), radical surgical excision has been the most effective (1). Clinical follow-up results have shown that complete resection of LAE lesion regions during surgery can ensure nonrecurrence and achieve radical cure (2). Hepatic surgical radical resection usually requires the resection range to be 1 cm over the lesion edge (2); however, since LAE lesions usually have no envelope, and the boundaries between the lesions and the normal liver tissues may not be obvious, surgical LAE lesion resection based on visual observation can leave residual lesions, resulting in the high likelihood of disease recurrence following surgery (3). A diagnosis of LAE and LAE lesion boundaries should be confirmed preoperatively. For patients with LAE that cannot undergo radical liver resection, evaluating such biological characteristics as the proliferation and invasion of lesions is important so that an appropriate alternative treatment plan can be made (4).

A previous study (5) showed that the increased uptake of ^{18}F-fluorodeoxyglucose (^{18}F-FDG) was not only associated with tumor cell proliferation and increased hypoxia-induced glycolysis, but also with gene mutations of various tumors during signal transduction, which resulted in the inhibition of apoptosis and oxidative phosphorylation and the activation of glycolysis; therefore, *in vivo* molecular imaging examination can determine the biological target regions of tumors, and the imaging can be used to guide clinical diagnosis and treatment. Another study confirmed that the biological behavior of LAE lesions was similar to that of tumors, including peri-LAE lesion neovessels and hepatocellular apoptosis (6). In terms of chronic inflammation, ^{18}F-FDG accomplished the imaging diagnosis primarily by identifying the notably increased energy demand of active-energy metabolism inflammatory cells and proliferated fibroblasts, among others. Reuter *et al* (7) used positron emission tomography (PET) to follow the metabolic changes of ^{18}F-FDG inside LAE lesions and found that when the edge of the focal liquefaction zone retained the sparse reduction of radionuclides, the lesion would be relatively stable; however, when radionuclides on the edge of the focal liquefaction zone progressed from sparse reduction to local

accumulation, the invasive progress of the lesions increased, and the 'proliferation and infiltration band' on the lesion edges or the active lesion region was recognized as important indicator of the development of lesions. Peri-LAE tissue-bioactive regions that exhibited different energy metabolisms and redefined biological boundaries of the lesions revealed the clinical significance of recognizing the LAE infiltration mechanism in the surrounding hepatic tissues.

As a treatment option for advanced LAE, autologous liver transplantation (ALT) has been increasingly carried out in recent years. Effectively determining the indications and surgical timing for LAE-ALT and detecting post-ALT recurrence and metastasis as early as possible is the significant clinical value of ALT as a treatment for LAE (8). *In vitro*, hepatic resection plus ALT could be an ideal choice for end-stage LAE radical treatment. ^{18}F-FDG PET/computed tomography (CT) can reveal more biological characteristics of the lesions, the tissue cells of the lesion limbic region and the associated development and outcomes. Multiple factors post-ALT can easily lead to LAE recurrence and distant metastasis. ^{18}F-FDG PET/CT can assist in the early detection and assessment of post-ALT hepatic functional status, as well as the recurrence or risk of metastasis. The present study reviews the clinical data, radiological information and follow-up associated with the use of ^{18}F-FDG PET/CT in 8 LAE-ALT patients, with the aim of evaluating its value in preoperative evaluation and prognosis determination.

Materials and methods

Clinical data. Eight patients with LAE, who were treated in the First Affiliated Hospital of Xinjiang Medical University (Urumqi, China) between December 2010 and December 2013, were selected for this study. The patients included 3 males and 5 females with an average age of 36±14 years. This study was conducted in accordance with the Declaration of Helsinki and with approval from the Ethics Committee of Xinjiang Medical University. Written informed consent was obtained from all participants. All patients underwent echinococcosis serological examination, with 8 positive results that were confirmed by postsurgical echinococcosis histopathological examination. All patients were treated by *in vitro* hepatic resection plus ALT. The LAE diagnoses in this study were between benign and malignant, growth was relatively slow and the compensatory hyperplasia of the healthy liver met the need for transplantation. The normal liver mass in these patients with LAE was 860±350 g after a half year of rest.

^{18}F-FDG-PET/CT imaging protocol and image interpretation. The Discovery VCT PET/CT (GE Healthcare Bio-Sciences, Pittsburgh, PA, USA) was used with an ^{18}F-FDG tracer produced by Cyclotron (GE Healthcare Bio-Sciences) that had a radiochemical purity of >95%. Prior to the PET/CT examination, patients fasted for 4-6 h to achieve a fasting blood glucose of <7 mmol/l. Patients were intravenously injected with ^{18}F-FDG (7.4 MBq/kg body weight); 30 min after the injection, the patients drank 1,000 ml water. Following bladder emptying 1 h later, the patients drank another 300 ml water to fill the gastrointestinal tract. The PET/CT imaging followed.

The positioning image was performed first to determine the scanning range, which was from the top of the cranium to the mid-upper segment of the thighbone. The CT image acquisition parameters were as follows: Voltage, 120 kV; tube current, 260 mA; detector collimation, 64x0.625 mm; layer thickness, 3.75 mm; interlayer spacing, 3.75 mm; 0.6 msec/rotation; detector pitch, 0.983; and scanning time, 20-30 sec. The patient was told to breathe calmly. The three-dimensional PET acquisition was performed with the same scanning range as the CT, generally with 6-8 bed positions. Data for each bed position were collected for 3 min. Following collection, the CT data were applied to perform attenuation corrections for the PET images. The ordered subset expectation maximization iterative method was used to reconstruct the images of the cross-sectional, coronal and sagittal planes, as well as the PET-CT fusion images. All patients were treated with standard ^{18}F-FDG-PET/CT acquisition (i.e., PET/CT acquisition was performed 1 h after ^{18}F-FDG injection; the delayed ^{18}F-FDG-PET/CT acquisition was performed 2 h after ^{18}F-FDG injection).

The early and delayed images of the patients were collected; image diagnosis was carried out by experienced physicians in the Department of Nuclear Medicine at the First Affiliated Hospital of Xinjiang Medical University, and the PET, CT and PET/CT fusion images were independently analyzed. First, image quality was determined by visual analysis, allowing normal physiological uptake, as well as normal variations and artifacts, to be standardized. Next, the abnormal radiopharmaceutical accumulation and biological borders of the lesions, and the numbers and measurements of the maximum standardized uptake value (SUVmax) accumulated in these lesions were recorded. According to the anatomical information provided by the same CT machine, the position of each lesion was then precisely identified.

All patients underwent surgery, and pathological sectioning was performed on the diseased tissues; a pathologist analyzed the slices.

Statistical analysis. SPSS 16.0 software (SPSS, Inc., Chicago, IL, USA) was used for the statistical analysis, and the measurement data are expressed as the mean ± standard deviation. The biological boundaries of LAE and the ALT-SUVmax were measured, and the data were analyzed by two-sample t-tests. The diagnostic performance analysis of the ^{18}F-FDG-PET/CT LAE biological boundary was determined by the χ^2 test, with $P<0.05$ considered to be a significant difference.

Results

Preoperative LAE-ALT assessment. The 8 patients with LAE had a total of 17 hepatic lesions, among which 12 were in the right lobe, 5 were in the left and 3 were extrahepatic. The mean LAE lesion diameter was 6.85±4.35 cm.

The LAE liver morphologies were disordered, the ratio of hepatic lobes was imbalanced, the outlines were incomplete, partial liver structures were missing, the radioactivity distribution inside the liver parenchyma was uneven and there were various degrees of disease involvement in the hepatic boundaries. Ten LAE lesions exhibited points of calcification that all were located in the central part of the lesions. Five

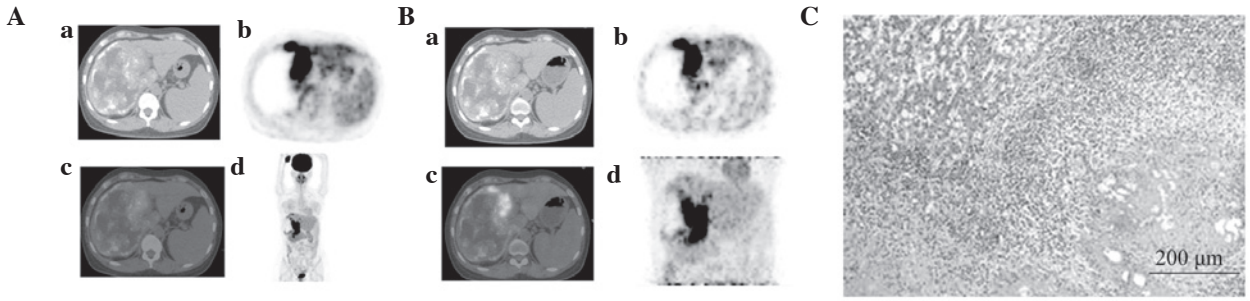

Figure 1. Whole-body positron emission tomography (PET)/computed tomography (CT) imaging. (A) (a) Hepatic right lobe exhibited a mixed space-occupying lesion with multiple scattered, spotty calcification lesions and regions of liquefactive necrosis, as detected by CT; (b) A region with significant radiopharmaceutical distribution was noted at the right anterior segment of hepar, as detected by PET; (c) A region with significant radiopharmaceutical distribution was noted at the junction of the hepatic right and left lobes; the shape was irregular and there was high radiopharmaceutical up take, as detected by PET/CT fusion imaging; (d) A region with significant radiopharmaceutical distribution was noted at the hepatic right lobe, as detected by MIP. (B) (a) The hepatic right lobe exhibited a mixed space-occupying lesion with multiple scattered, spotty calcification lesions and regions of liquefactive necrosis, as detected by CT; (b) The radiopharmaceutical accumulation was significantly enhanced, as compared with the earlier image, and standardized uptake value (SUV) was increased, as detected in the PET delayed image; (c) A region with significant radiopharmaceutical distribution was noted at the junction of the hepatic right and left lobes, and the radiopharmaceutical accumulation was significantly enhanced, as detected in the PET/CT fusion delayed image; (d) The radiopharmaceutical accumulation was significantly enhanced, as compared with the earlier image, and SUV was increased at the hepatic right lobe, as detected in the MIP delayed image. (C) Between the coagulation of necrotic and normal liver tissue, fibroblast proliferation and lymphocyte, plasma cell and eosinophil infiltration could be observed, forming the inflammatory fibrous tissue band (HE staining). MIP, maximum intensity projection.

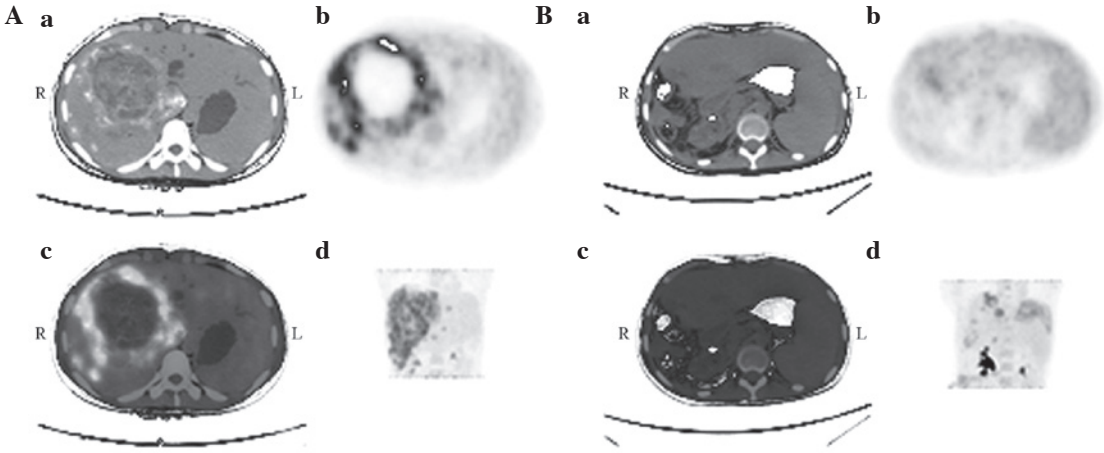

Figure 2. Comparison of whole-body positron emission tomography (PET)/computed tomography (CT) images (A) prior to and (B) following autologous liver transplantation. (A) (a) Hepatic right lobe exhibited a mixed space-occupying lesion with multiple scattered, spotty calcification lesions and regions of liquefactive necrosis, as detected by CT; (b) A cycle with significant and uneven radiopharmaceutical distribution was noted at the the hepatic right lobe, as deteceted by PET; (c) A cycle with significant and uneven radiopharmaceutical distribution was noted at the hepatic right lobe, the shape was irregular and there was high radiopharmaceutical uptake, as detected by PET/CT fusion imaging; (d) A lump-like and uneven significant radiopharmaceutical distribution was noted at the hepatic lobes, as detected by MIP. (B) (a) The density of autologous transplanted liver was uniform, as detecetd by CT; (b) Radiopharmaceutical distribution was uniform, as detected by PET; (c) Radiopharmaceutical distribution was uniform in autologous transplanted liver, as detected by PET/CT fusion imaging; (d) Radiopharmaceutical distribution was uniform in autologous transplanted liver, as detected by MIP. MIP, maximum intensity projection.

patients exhibited obvious abnormalities in the porta hepatis, and 3 exhibited extrahepatic bile duct involvement. The lesions were all mixed space-occupying lesions and most had irregular shapes. The LAE lesion boundaries were unclear and infiltrated tissues; the peri-lesion boundaries could be outlined through the radiopharmaceutical intake. Focal radiopharmaceutical distribution presented as an enhanced distribution of radioactivity on the partial edges, suggesting that the focal lesions were in the proliferative growth or LAE active period (Fig. 1).

The radiopharmaceutical intake in the peri-lesion tissues was significant, possessing the characteristics of radiopharmaceutical-outlined borders and exhibiting border-increased radiopharmaceutical intake. The SUVmax value of the patients was 3.57±1.21 and exhibited the characteristics of biological activity (Fig. 1). Radiopharmaceutical fading did not occur in the 2-h delayed images, whereas the radioactivity distribution was more enhanced than the previous ^{18}F-FDG uptake. The SUVmax in the delayed images was 4.19±1.70 overall, and each lesion exhibited various degrees of increased SUV (Fig. 2).

The patients underwent surgical excision of the lesions, and the resected lesions were sent to the pathology department for slicing and staining. The results of the pathological diagnoses were as follows: i) Hepatic steatosis/hepatic sinusoid dilatation and congestion; ii) inflammatory band around the liver cells; iii) echinococcosis with *Echinococcosis multilocularis*; iv) calcified lesions of

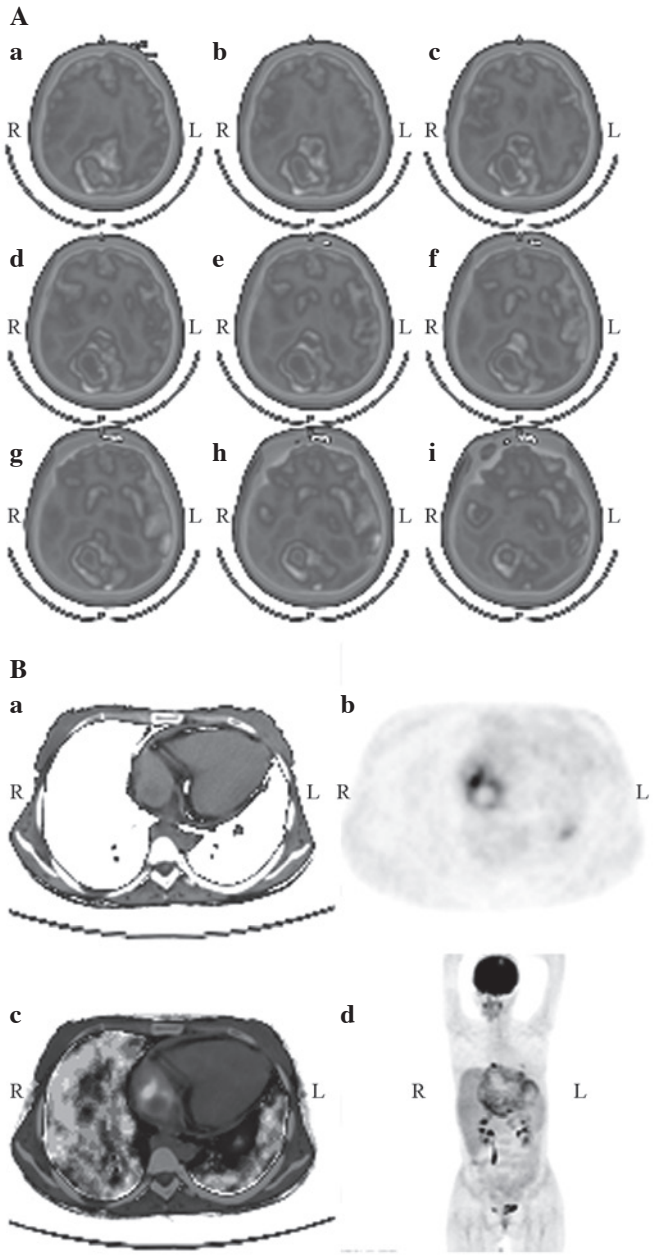

Figure 3. Positron emission tomography (PET)/computed tomography (CT_ imaging was used to visualize liver alveolar echinococcosis extrahepatic metastasis. (A) (a-i) Brain metastasis in right occipital lobe. (B) (a) A mixed space-occupying (AE) at right atrium, as detected by CT; (b) A cycle with significant and uneven radiopharmaceutical distribution was noted at right atrium, as detected by PET; (c) Radiopharmaceutical distribution was uniform in the autologous transplanted liver, as detected by PET/CT fusion imaging; (d) Radiopharmaceutical distribution was uniform in the autologous transplanted liver, as detected by MIP. MIP, maximum intensity projection.

echinococcosis; v) fibrous inflammatory band/infarct zone; vi) small bile duct hyperplasia; vii) inflammatory band; and viii) normal/fibrous inflammatory band/echinococcosis region.

The SUV of the LAE-normal liver areas was 0.95±0.19 overall. Among the 8 patients with LAE, 3 exhibited a significant extrahepatic radiopharmaceutical uptake area; specifically, the gyrus rectus of the right brain, right atrium and both lungs exhibited biologically active LAE lesions (Fig. 3). The SUVmax value was 2.05±0.72 and the SUVmax of the delayed imaging was 3.15±0.83, indicating LAE extrahepatic invasion and a proliferating or active period of LAE.

Table I. Statistics of PET/CT diagnosis and pathological diagnosis.

	Pathological diagnosis (standard diagnosis)		
PET/CT diagnosis	+	-	Total
+	11	2	13
-	1	3	4
Total	12	5	17

Sensitivity, 91.67%; specificity, 60.00%; accuracy, 82.35%; positive predictive value, 84.62%; negative predictive value, 75.00%. PET/CT, positron emission tomography/computed tomography.

Diagnostic PET/CT LAE test analysis. Pathological diagnosis was performed on the 17 lesions, and SPSS 17.0 software was used to determine the statistical analyses of the biopsy results. The PET/CT images, PET/CT-based LAE biological borders and pathological lesion boundaries determined the diagnostic test analyses with a corresponding fourfold table. The statistical analyses of the pathological results and PET/CT diagnostic results are shown in Table I.

Post-ALT assessment

Assessment of liver survival status following LAE-ALT. The SUVmax value of patients 1 month after LAE-ALT was 1.23±0.78; the values after 3 and 6 months were 1.15±0.67 and 0.85±0.35, respectively. Compared with the normal liver SUV value (0.95±0.19), the 1-month SUV value exhibited a statistically significant difference. All LAE-ALT patients were followed for 1-39 months, and no new occurrence of extrahepatic LAE metastasis was found.

Biological activities of post-LAE-ALT extrahepatic metastatic lesions. The SUVmax value of the extrahepatic metastatic lesions 3 months after LAE-ALT was 1.85±0.62 and the delayed imaging SUVmax at the same time-point was 2.95±0.79. These values exhibited no significant difference from the preoperative values.

Discussion

Since LAE cannot be easily detected in the early clinical stage, *Echinococcus* parasites have typically already widely invaded intrahepatically and extrahepatically when obvious liver function impairment is found (8,9). As a result, the radical resection rate associated with LAE has been low (10), and, if the condition is not treated, the 10-year mortality rate can be as high as 93%. LAE causes much more harm to the human body than does cystic hydatid disease, and thus it has been referred to as the 'worm cancer' (11).

Currently, among the LAE treatment methods, only radical surgical excision has shown notable efficacy. Clinical follow-up results have revealed that the complete removal of

LAE lesions can ensure no recurrence and radical cure (12). For those patients in whom radical liver resection is not an option, evaluating the proliferation and invasion of lesions is important for an appropriate treatment plan.

According to the distribution and distribution characteristics of positron radiopharmaceuticals, the associations and pathological relationships with other suspicious lesions can be diagnosed and, thus, the positive boundary edges between the LAE lesions and normal liver tissues can be more accurately exhibited (13). Within the 8 LAE cases in this study, there were 17 lesions, with 12 on the right lobe and 5 on the left. The overall LAE lesion diameter was 6.85±4.35 cm. The radiopharmaceutical uptake around the LAE lesions was significant and exhibited increased radiopharmaceutical-outlined borders. The overall SUV value was 3.57±1.21 and indicated bioactive characteristics. The 2-h delayed image did not indicate fading radiopharmaceutical uptake, and the radioactivity distribution was more enhanced than the previous ^{18}F-FDG uptake. The SUV of the delayed image was 4.19±1.70 overall, and each lesion exhibited different degrees of increased SUV. Postoperative pathology confirmed the diagnosis of LAE and an inflammatory tissue band, similar to that described by Caoduro *et al* (14).

Following the study of LAE for 30 years, Wen *et al* (15) successfully completed the LAE-ALT procedure. Due to limited intrahepatic lesions and no extrahepatic metastasis, 90% of patients with early LAE can be cured, but most patients are in the end stages of disease when diagnosed; therefore, only 35% of patients have the option of radical surgery.

As a result of the late diagnosis of LAE, liver transplantation has become the only treatment method for end-stage LAE. LAE recurrence and metastasis are key factors that influence the long-term outcomes of liver transplantation (16). A lower dose of immunosuppressive drugs following transplantation, as well as the long-term, systemic administration of anti-LAE drugs, is important to prevent and reduce LAE recurrence and metastasis. *In vitro* liver resection plus ALT is an ideal choice for end-stage LAE radical treatment (17,18). The significance of the evaluation efficacy of PET/CT in LAE-ALT has made the biological characteristics of LAE lesions clear prior to surgery; it is now possible to evaluate whether invasion has occurred in other organs prior to surgery.

In order to determine the probabilities of the occurrence post-ALT recurrence and metastasis of LAE, PET/CT can simultaneously enable observation of the morphology and metabolism of all body tissues and reveal the biological characteristics of the transplanted liver. In this study, the SUVmax value of liver surviving 1 month after LAE-ALT was 1.23±0.78, and that of liver surviving after 3 and 6 months was 1.15±0.67 and 1.03±0.06, respectively. Compared with that of normal liver, the 1-month SUVmax value exhibited a statistically significant difference, suggesting that the post-ALT surviving liver exhibited dynamic ^{18}F-FDG metabolic changes. In the first month the ^{18}F-FDG uptake indicated high metabolic changes, but these stabilized 2 months later, which was similar to the ^{18}F-FDG metabolism of the normal liver. All LAE-ALT patients were followed up for 1-39 months, with the exception of 1 patient with LAE extrahepatic metastasis, and this reflects the ideal radical surgical treatment towards end-stage LAE.

Among the 8 patients in this study, 3 exhibited significant extrahepatic radiopharmaceutical uptake on the gyrus rectus of the right side of the brain, the right atrium or both the lungs, which showed bioactive LAE lesions (SUVmax, 2.05±0.72; delayed imaging SUVmax, 3.15±0.83), indicating that ALT did not change the biological activities of the extrahepatic lesions of LAE.

Controversy remains, both in China and elsewhere, about the selection of indications and timing of LAE-ALT. Bresson-Hadni *et al* (19,20) believed that patients with end-stage LAE that are unable to undergo this surgical treatment should be added to the liver transplantation waiting list. It has also been suggested that preoperative brain metastasis should be classified as a contraindication to surgery, whereas lung metastasis has not been classified as a contraindication (21). From the results of the current study, ALT should still be considered the ideal treatment method, even in the presence of extrahepatic metastasis. As the SUVmax value of the post-ALT extrahepatic metastatic lesions was 1.85±0.62 and the delayed imaging SUVmax exhibited no significant difference from the value prior to transplantation, this study could provide an important basis for selecting the indications and surgical timing of LAE-ALT.

Acknowledgements

This study was supported by the Natural Science Foundation of Xinjiang Uygur Autonomous Region (grant nos. 2012211A0 and 2012211A081).

References

1. Silva MA, Mirza DF, Bramhall SR, Mayer AD, McMaster P and Buckels JA: Treatment of hydatid disease of the liver. Evaluation of a UK experience. Dig Surg 21: 227-233, 2004.
2. Parsak CK, Demiryurek HH, Inal M, *et al*: Alveolar hydatid disease: Imaging findings and surgical approach. Acta Chir Belg 107: 572-577, 2007.
3. Gollackner B, Längle F, Aner H, *et al*: Radical surgical therapy of abdominal cystic hydatid disease: Factors of recurrence. World J Surg 24: 717-721, 2000.
4. Hosch W, Junghanss T, Werner J and Düx M: Imaging methods in the diagnosis and therapy of cystic echinococcosis. Rofo 176: 679-687, 2004 (In German).
5. Lee JW, Paeng J, Kang KW, *et al*: Prediction of tumor recurrence by ^{18}F-FDG PET in liver transplantation for hepatocellular carcinoma. J Nulc Med 50: 682-687, 2009.
6. Pichler BJ, Kneilling M, Haubner R, Braumüller H, Schwaiger M, Röcken M and Weber WA: Imaging of delayed-type hypersensitivity reaction by PET and 18F-galacto-RGD. J Nucl Med 46: 184-189, 2005.
7. Reuter S, Grüner B, Buck AK, Blumstein N, Kern P and Reske SN: Long-term follow-up of metabolic activity in human alveolar echinococcosis using FDG-PET. Nuklearmedizin 47: 147-152, 2008.
8. Charbonnet P, Buhler L, Sagnak E, Villiger P, Morel P and Mentha G: Long-term follow up of patients with alveolar echinococcosis. Ann Chir 129: 337-342, 2004 (In French).
9. Bauder B, Auer H, Schilcher F, Gabler C, Romig T, Bilger B and Aspöck H: Experimental investigations on the B and T cell immune response in primary alveolar echinococcosis. Parasite Immunol 21: 409-421, 1999.
10. Tang QK, Zhang Z, Li YS, Yuan CP and Zhang DT: Analysis on treatment of liver alveolar hydatid disease. Ji Sheng Chong Yu Gan Ran Xing Ji Bing 4: 19-20, 2006 (In Chinese).
11. Wen H and Xu M (eds.): Practical Echinococcosis. Science Press, Beijing, pp 226-227, 2007.
12. Manus DP, Zhang W, Li J and Bartley PB: Echinococcosis. Lancet 362: 1295-1304, 2003.
13. Bostanci B, Tetik C, Terzi C and Ozden A: Efficiency of ultrasound in the detection of the viability of hydatid cysts in the liver. Surg Laparosc Endosc Percutan Tech 9: 392-394, 1999.

14. Caoduro C, Porot C, Vuitton DA, *et al*: The role of delayed ^{18}F-FDG PET imaging in the follow-up of patients with alveolar echinococcosis. J Nucl Med 54: 358-363, 2013.
15. Wen H, Zuo MX, Wang XY, *et al*: The first human liver transplantation of alveolar echinococcosis in China. Zhong Hua Xiao Hua Wai Ke Za Zhi 23: 375, 2002 (In Chinese).
16. Yüksel O, Akyürek N, Sahin T, Salman B, Azili C and Bostanci H: Efficacy of radical surgery in preventing early local recurrence and cavity-related complications in hydatic liver disease. J Gastrointest Surg 12: 483-489, 2008.
17. Zhang L, Zhang SJ, Cao YW, *et al:* The correlation between osteopontin and metastasis of hepatic *Echinococcus* multilocularis infection. Zhongguo Ji Sheng Chong Xue Yu Ji Sheng Chong Bing Za Zhi 29: 33-36, 2011 (In Chinese).
18. Elsebaie SB, El-Sebae MM, Esmat ME, Nasr MM and Kamel MM: Modified endocystectomy versus pericystectomy in *Echinococcus granulosus* liver cysta: A randomized controlled study and the role of specific anti-hydatid IgG4 in detection of early recurrence. J Egypt Soc Parasitol 36: 993-1006, 2006.
19. Bresson-Hadni S, Vuitton DA, Bartholomot B, *et al*: A twenty-year history of alveolar echinococcosis: analysis of a series of 117 patients from eastern France. Eur J Gastroenterol Hepatol 12: 327-336, 2000.
20. Bresson-Hadni S, Mignet JP, Lenys D, *et al*: Recurrence of alveolar echinococcosis in the liver graft after liver transplantation. Hepatology 16: 279-280, 1992.
21. Czemak BV, Akhan O, Hiemetzberger R, *et al*: Echinococcosis of the liver. Abdom Imaging 33: 133-143, 2008.